Developmental Biology 323 (2008) 31–40

Contents lists available at ScienceDirect

Developmental Biology

journal homepage: www.elsevier.com/developmentalbiology

The *orphan G protein-coupled receptor 161* is required for left–right patterning

TinChung Leung [a,*], Jasper E. Humbert [a], Anna M. Stauffer [a], Kathryn E. Giger [a], Hui Chen [a], Huai-Jen Tsai [b], Chuan Wang [a], Tooraj Mirshahi [a], Janet D. Robishaw [a,*]

[a] *Weis Center for Research, Geisinger Clinic, Danville, PA 17822, USA*
[b] *Institute of Molecular and Cellular Biology, National Taiwan University, Taipei, Taiwan*

ARTICLE INFO

Article history:
Received for publication 10 March 2008
Revised 28 July 2008
Accepted 1 August 2008
Available online 7 August 2008

Keywords:
Orphan GPCR
Ca^{2+}
Left–right asymmetry
Cardiac looping
Visceral asymmetry
Zebrafish development

ABSTRACT

Gpr161 (also known as RE2) is an orphan G protein-coupled receptor (GPCR) that is expressed during embryonic development in zebrafish. Determining its biological function has proven difficult due to lack of knowledge regarding its natural or synthetic ligands. Here, we show that targeted knockdown of *gpr161* disrupts asymmetric gene expression in the lateral plate mesoderm, resulting in aberrant looping of the heart tube. This is associated with elevated Ca^{2+} levels in cells lining the Kupffer's vesicle and normalization of Ca^{2+} levels, by over-expression of *ncx1* or *pmca*-RNA, is able to partially rescue the cardiac looping defect in *gpr161* knockdown embryos. Taken together, these data support a model in which *gpr161* plays an essential role in left–right (L–R) patterning by modulating Ca^{2+} levels in the cells surrounding the Kupffer's vesicle.

Introduction

G protein-coupled receptors (GPCRs) are emerging as critical regulators of diverse developmental processes such as oocyte maturation (Romo et al., 2008), fertilization (Fraser et al., 2003), gastrulation (Lin et al., 2005), and organogenesis (Griffin et al., 2001; Kupperman et al., 2000; Leung et al., 2006; Offermanns et al., 1997; Ruppel et al., 2005; Scott et al., 2007; Zeng et al., 2007). However, there is limited information regarding the embryonic expression patterns and functions of the ~400 non-olfactory GPCRs identified in the human and mouse genomes (Fredriksson et al., 2003; Vassilatis et al., 2003). Zebrafish offer a number of advantages for undertaking this type of large-scale analysis (Amsterdam et al., 1999; Driever et al., 1996; Geisler et al., 2007; Haffter et al., 1996; Peterson et al., 2000). The expression patterns of the individual GPCRs can be quickly determined by whole mount in situ hybridization, while their functions can be rapidly surveyed by visual inspection of the knockdown phenotypes resulting from morpholino antisense oligonucleotide (MO) injection (Nasevicius and Ekker, 2000). Particularly relevant to this study, zebrafish are very suitable for studying cardiac development since the embryos develop externally and do not require blood circulation for their early development, thereby allowing even those embryos showing severe cardiac defects to be analyzed in detail. Understanding the molecular basis for such cardiac defects is important for long term prevention of congenital heart problems that represent the most common of all human birth defects and affect nearly 1% of the population.

The formation of a fully functional heart is a multi-step process (Yelon et al. 1999). It begins with the specification of the appropriate numbers of myocardial cells within the lateral plate mesoderm (LPM). As myocardial differentiation progresses, the bilateral clusters of myocardial cells migrate medially and merge at the embryonic midline. As myocardial elongation occurs, the heart tube undergoes a complex series of morphogenetic movements in which the tube initially jogs to the left at 24 hpf (hour-post-fertilization) and then loops to the right between 30 and 48 hpf to form the functional, two-chambered heart. In the present study, we exploited zebrafish as a model system to investigate the role of a newly discovered orphan GPCR in this process. Using a combination of whole mount in situ hybridization and antisense morpholino oligonucleotide (MO) knockdown approach, we show that *gpr161* is normally expressed in the lateral plate mesoderm and that knockdown of its expression perturbs cardiac looping as the result of a defect in left–right (L–R) patterning. This study reveals an essential role for a GPCR in L–R patterning for the first time and also adds to a growing list of GPCRs known to have critical roles during development (Kupperman et al., 2000; Scott et al., 2007; Zeng et al., 2007).

* Corresponding authors. Fax: +1 570 271 6701.
E-mail addresses: tleung1@geisinger.edu (T. Leung), jrobishaw@geisinger.edu (J.D. Robishaw).

0012-1606/$ – see front matter © 2008 Elsevier Inc. All rights reserved.
doi:10.1016/j.ydbio.2008.08.001

Results

The orphan G protein-coupled receptor 161 is expressed in the developing zebrafish embryos

The human orphan receptor *RE2* was originally isolated from fetal brain (Genbank accession AF091890; http://www.ncbi.nlm.nih.gov) and was later renamed *GPR161* as a member of the GPCR superfamily (reference sequence NM_153832). Following a large-scale phylogenetic analysis, the human *GPR161* was assigned to the δ group of the *RHODOPSIN* family within the purine receptor cluster that includes several known receptors that bind such diverse ligands as nucleotides, leukotrienes, and thrombin (Fredriksson et al., 2003). However, nearly ten years after its initial discovery, the natural ligand and biological function of the human *GPR161* remain to be discovered.

To search for the zebrafish ortholog, we used the human *GPR161* gene to query the zebrafish genomic sequence databases and identified several contigs containing portions of the candidate gene. We subsequently generated a full length zebrafish *gpr161* cDNA by reverse transcription-polymerase chain reaction (RT-PCR) for further analysis. Translation of the open-reading frame predicted a 526-amino acid protein that showed 77% overall similarity to the human GPR161 protein. Since the *RHODOPSIN* family members typically bind their ligands via their seven transmembrane (7TM) domains (Schwartz et al., 2006), sequence alignments of the 7TM domains are often more insightful for making cross-

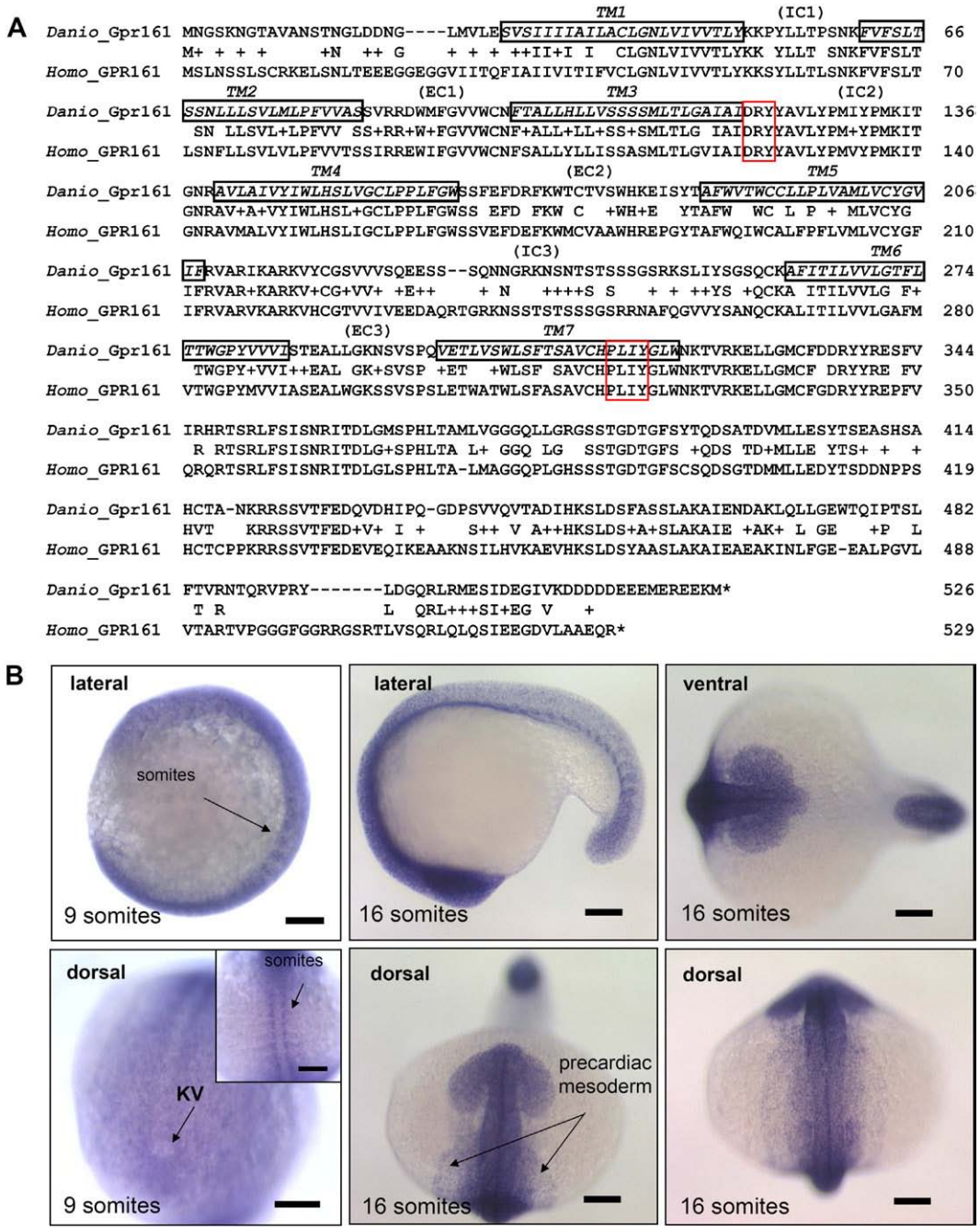

Fig. 1. Sequence comparison and in situ expression analysis of zebrafish *gpr161*. (A) Genbank accession no. of human *GPR161*: NM_007369 (*Homo*); zebrafish *gpr161*: EU090912 (*Danio*). 7TM (black), DRY (red) and PxxY (red) motifs were boxed. (B) *gpr161* expression in the developing embryos by whole mount in situ hybridization. Inset showed the expression in developing somites and expression surrounding the Kupffer's vesicle (KV) near the tail bud region at 9-somite stage. All scale bars were 100 μm.

species comparisons (Fredriksson and Schioth 2005). Using the hidden Markov model (Krogh et al., 2001) (TMHMM Server v. 2.0, http://www.cbs.dtu.dk/services/TMHMM/) to identify the 7TM domains (Fig. 1A; Supplementary Figs. 1A–C), the 7TM regions of the zebrafish Gpr161 protein showed a remarkable 86% overall similarity to the human GPR161 protein, providing evidence of their close evolutionary relationship and further suggesting their ligand binding function has been conserved from fish to man. Further comparison of the two protein sequences revealed other obvious similarities (Fig. 1A; Supplementary Figs. 1A–C). The most conserved regions were found on the inner face of the cell membrane, including the intracellular IC2 loop (100% similarity); the DRY motif at the border between TM3 and IC2 loop; the IC3 domain (71% homology); the PxxY motif in the TM7 domain, and the proximal portion of the C-terminal tail (84% similarity). Such high sequence homology between these proteins, particularly in the IC loops and the proximal portion of the C-terminal tail, indicated that the G protein coupling function of the predicted zebrafish and human GPR161 proteins has been evolutionarily conserved. By contrast, the more diverse regions were located on the outer face of the cell membrane, including the N-terminus and the three extracellular EC loops. Presumably, there was no strong evolutionary pressure to conserve these sequences since they are not predicted to mediate ligand binding or G protein activation (Möller et al., 2001). Thus, extensive sequence comparisons suggest the zebrafish gene is the ortholog of the human *GPR161* gene (Fig. 1A; Supplementary Figs. 1A–C). This is further supported by phylogenetic analysis within the purine receptor cluster branch (Fredriksson et al., 2003) (Supplementary Fig. 2A).

Much can be learned about the possible functions of *GPR161* from examination of its expression profile. ESTs for human *GPR161* were identified in brain, colon, heart, lung, prostate, salivary gland, skin, mouth and uterus libraries (NCBI Expression Profile of Unigene Hs.632453 at http://www.ncbi.nlm.nih.gov/UniGene/). Using a combination of RT-PCR analysis (Supplementary Fig. 2B) and whole mount in situ hybridization (Fig. 1B; Supplementary Fig. 2C), we showed that zebrafish *gpr161* transcripts were expressed throughout embryonic development. At earlier stages (9- to 16-somites), *gpr161* transcripts were broadly expressed with specific staining observed in the developing nervous system, somites, and precardiac mesoderm (Fig. 1B; compare to negative control in Supplementary Fig. 2D). At later stages (1- to 3-days post-fertilization (dpf)), transcripts became more localized within the dorsal diencephalon, the otic vesicles, and the fin buds (Supplementary Fig. 2C). This dynamic expression pattern suggests important roles for zebrafish *gpr161* throughout embryonic development.

Genetic manipulation of zebrafish gpr161 disrupts embryonic development

To investigate how zebrafish *gpr161* may function in embryonic development, we used a morpholino antisense oligonucleotide (MO) approach to knockdown *gpr161* in developing zebrafish embryos (Nasevicius and Ekker, 2000; Leung et al., 2006). To confirm the sequence specificity of any observed defects, two morpholinos targeted against different regions of the 5′UTR of the zebrafish *gpr161* mRNA were used (Supplementary Fig. 3A). As validated by the in vitro translation assay, both *gpr161*-MOs (MO#24 and MO#36) inhibited expression of the zebrafish Gpr161 protein in a dose dependent fashion (Supplementary Figs. 3B, C). By contrast, a 5-base mismatch control MO (MO#28) failed to inhibit Gpr161 protein expression, attesting to the efficacy and sequence specificity of the knockdown approach (Supplementary Figs. 3B, C).

Following injection of either *gpr161*-MO (MO#24 or MO#36), transgenic embryos exhibiting heart specific fluorescence (*TG[cmlc:GFP]*) were collected from different stages and screened for morphological, molecular, and functional defects. This analysis revealed that the majority of the zebrafish *gpr161* knockdown embryos exhibited pericardial edema and improper juxtaposition of the atrium and

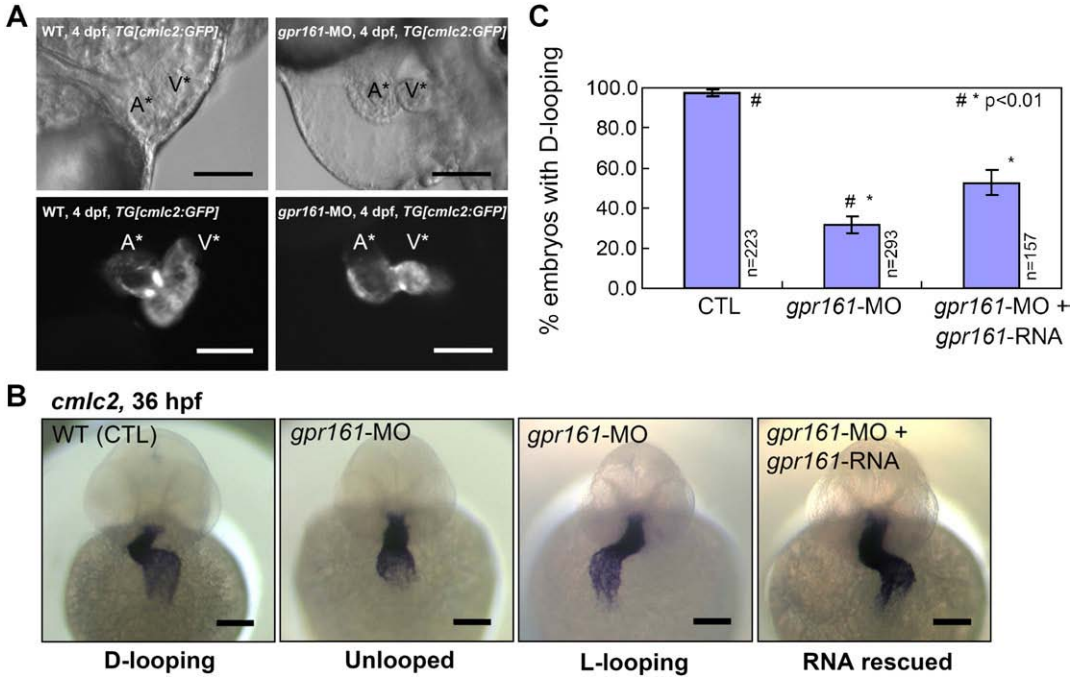

Fig. 2. *gpr161* knockdown disrupts cardiac looping morphogenesis. (A) Lateral view of zebrafish hearts at 4 dpf. Control and *gpr161* knockdown in transgenic zebrafish embryos with cardiac specific GFP, *TG[cmlc2:GFP]*, showing images of bright field (top panels) and fluorescent (bottom panels). A* labelled atrium, V* labelled ventricle. (B) Cardiac looping morphogenesis marked by *cmlc2* expression in control (D-looping), *gpr161* knockdown (unlooped and L-looping) and RNA rescued embryos. All scale bars were 100 μm. (C) Graphical summary of *gpr161* knockdown disrupted normal cardiac D-looping morphogenesis at 36 hpf. Calculation as % of embryos with D-looping in control (97.8±1.3%; $n=223$), embryos injected with *gpr161* morpholino (MO#36, 32.4±4.1%; $n=293$) and RNA rescue (*gpr161* RNA without 5′UTR; 52.2±3.4%; $n=157$), n was number of total embryos and results were from 4 injection experiments. Error bars were ±SEM. t-test * and # indicated statistical significance, $p<0.01$.

ventricle at 4 dpf (Fig. 2A). Attesting to specificity, the same phenotype was observed with both *gpr161*-MOs (Supplementary Fig. 3D). To investigate the underlying basis for this phenotype, we examined the expression of the cardiac specific marker, *cardiac myosin light chain 2 (cmlc2)* (Yelon et al., 1999), in zebrafish *gpr161* knockdown embryos (Fig. 2B). In control embryos, the *cmlc2* expressing cells form a linear heart tube around 25 hpf (data not shown) and the heart tube undergoes chamber maturation and normal looping of the ventricle to the right (D-looping) around 36 hpf (Fig. 2B). By contrast, aberrant looping of the ventricle was observed in a significant portion of *gpr161* knockdown embryos (Fig. 2B). Quantitative analysis of the observed phenotypes showed that 67.6% of *gpr161* knockdown embryos exhibited either no looping or abnormal looping of the ventricle to the left (L-looping), in contrast to 97.8% of the control embryos that underwent normal D-looping (Fig. 2C). Indicating an actual defect rather than a delay, the cardiac looping defect was still observed at 4 dpf (Fig. 2A). To further confirm that absent or aberrant L-looping was due to knockdown of zebrafish *gpr161*, we showed that the defect could be partially rescued by co-injection of *gpr161*-MO along with a morpholino resistant form of the zebrafish *gpr161*-RNA (open-reading frame without the 5′UTR targeted by the morpholino). Quantitative analysis showed that 52.2% of the embryos co-injected with *gpr161*-MO and -RNA displayed proper D-looping, compared to 32.4% injected with *gpr161*-MO alone (MO#36 at 5′UTR) (Fig. 2C; Supplementary Table 1). Consistent with the literature for other zebrafish genes (Ebert et al., 2005; Heisenberg et al., 2000), the lack of complete rescue is likely due to the inability of the injected *gpr161*-RNA to fully recapitulate the spatial and temporal expression of the endogenous gene. Collectively, these results indicate that zebrafish *gpr161* plays a critical role in cardiac looping.

Knockdown of zebrafish gpr161 disrupts L–R asymmetry

Failure to undergo cardiac looping is frequently the result of a defect in L–R patterning (Chen et al., 1997). One model for establishment of the L–R axis suggests the involvement of a ciliated organ known as the embryonic node in mice (Hirokawa et al., 2006) or Kupffer's vesicle in zebrafish (Oishi et al., 2006). Prior to formation of the heart tube, this organ is thought to produce a signal that leads to left-sided expression of several genes such as *lefty2* and *southpaw* (*spaw*) in the lateral plate mesoderm (LPM) in close proximity to the developing precardiac mesoderm (Essner et al., 2005; Chocron et al., 2007). To determine if loss of zebrafish *gpr161* disrupts L–R asymmetry, we first examined the expression of the *nodal* antagonists *lefty1 and lefty2* at 21 hpf. In control embryos, left-sided expression of *lefty1* (dorsal diencephalon) and *lefty2* (LPM) was detected in 99.3% of cases (Figs. 3A, B; Supplementary Table 2). By contrast, the left-sided expression of *lefty1* and *lefty2* was almost completely suppressed in 31.6% of *gpr161* knockdown embryos and was aberrant in 1.4% of embryos with bilateral or right-sided expression of *lefty2* in the LPM. Knockdown of *spaw* has been reported to perturb left-sided expression of *lefty2* and to disrupt cardiac looping in zebrafish embryos (Long et al., 2003). To determine if *spaw* expression was altered in *gpr161* knockdown embryos, we examined the expression of *spaw* at

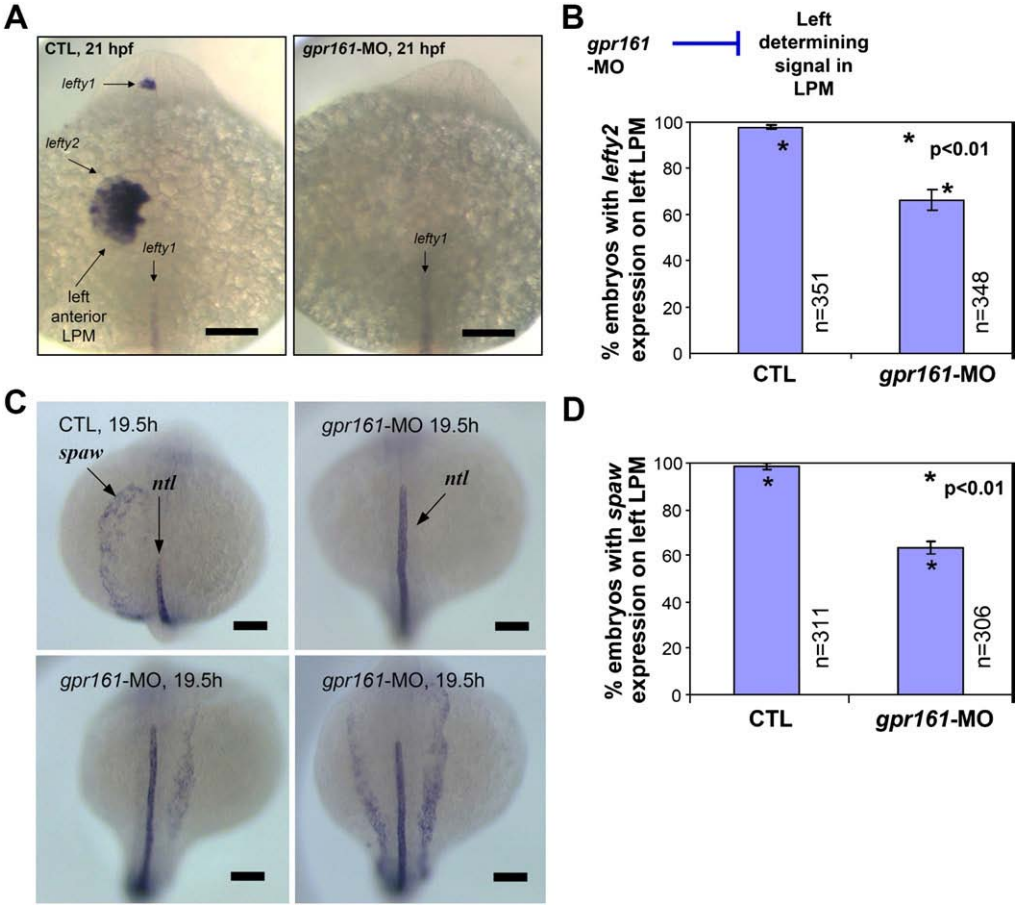

Fig. 3. *gpr161* knockdown disrupts L–R identity in lateral plate mesoderm. (A) *lefty2* expression in the left anterior lateral plate mesoderm (LPM) and *lefty1* expression in the left diencephalon were disrupted in *gpr161* knockdown embryos. (B) Graphical summary of control (99.3±1.1%; $n=351$), *gpr161* morpholino (MO#24, 67.0±4.7%; $n=348$) and *t*-test ($p<0.01$) results were from 11 injection experiments. (C) *spaw* expression in the left anterior lateral plate mesoderm (LPM) at 19.5 hpf in control and *gpr161* knockdown embryos. *ntl* expression marked the midline as a reference. (D) Graphical summary of *spaw* expression in control (98.7±1.4%; $n=311$), *gpr161* morpholino (MO#24, 63.4±2.7%; $n=306$) and *t*-test ($p<0.01$) results were from 13 injection experiments. Error bars were ±SEM. All scale bars were 100 μm.

an even earlier stage of somitogenesis (19.5 hpf). In control embryos, left-sided expression of *spaw* was detected in 98.7% of cases (Figs. 3C, D; Supplementary Table 3). By contrast, the left-sided expression of *spaw* was completely suppressed in 30.4% of *gpr161* knockdown embryos and was aberrant in 6.2% of knockdown embryos with either bilateral or right-sided expression of *spaw*. Demonstrating that altered *spaw* or *lefty2* expression was not due to a general disruption of the LPM, we showed that bilateral expression of *nkx2.5* (Chen and Fishman, 1996) in the precardiac mesoderm was not affected in *gpr161* knockdown embryos (Supplementary Fig. 4A). Also, ruling out a general disruption of the dorsal midline structures, we demonstrated that midline expression of *no tail* (*ntl*) (arrow in Fig. 3C) and *lefty 1* (arrow in Fig. 3A) was not altered in *gpr161* knockdown embryos. Collectively, these results demonstrate that L–R patterning in the LPM is specifically disrupted in the majority of *gpr161* knockdown embryos.

The *bmp4* gene, which encodes bone morphogenetic protein 4, is used as molecular marker of L–R asymmetry in the developing heart tube (Chen et al., 1997; Schilling et al., 1999). At 19 hpf (20-somite stage), *bmp4* is uniformly expressed in the cardiac cone. However, at 20 hpf (22-somite stage), the pattern of *bmp4* expression becomes asymmetric, with left-sided expression predominating over the right, immediately prior to the leftward jogging of the heart tube and subsequent looping to the right (Chen et al., 1997). As expected, at 23 hpf, 85.8% of control embryos preferentially expressed *bmp4* on the left side of the cardiac cone (Fig. 4A). By contrast, only 47.5% of *gpr161* knockdown embryos showed this pattern, with the rest of the embryos exhibiting similar levels of *bmp4* expression on both sides of the cardiac cone (Fig. 4A; Supplementary Table 4). Likewise, at 25 hpf, 99.5% of control embryos preferentially expressed *bmp4* on the left side of the developing heart tube compared to only 56.9% of *gpr161* knockdown embryos (Fig. 4B; Supplementary Table 4).

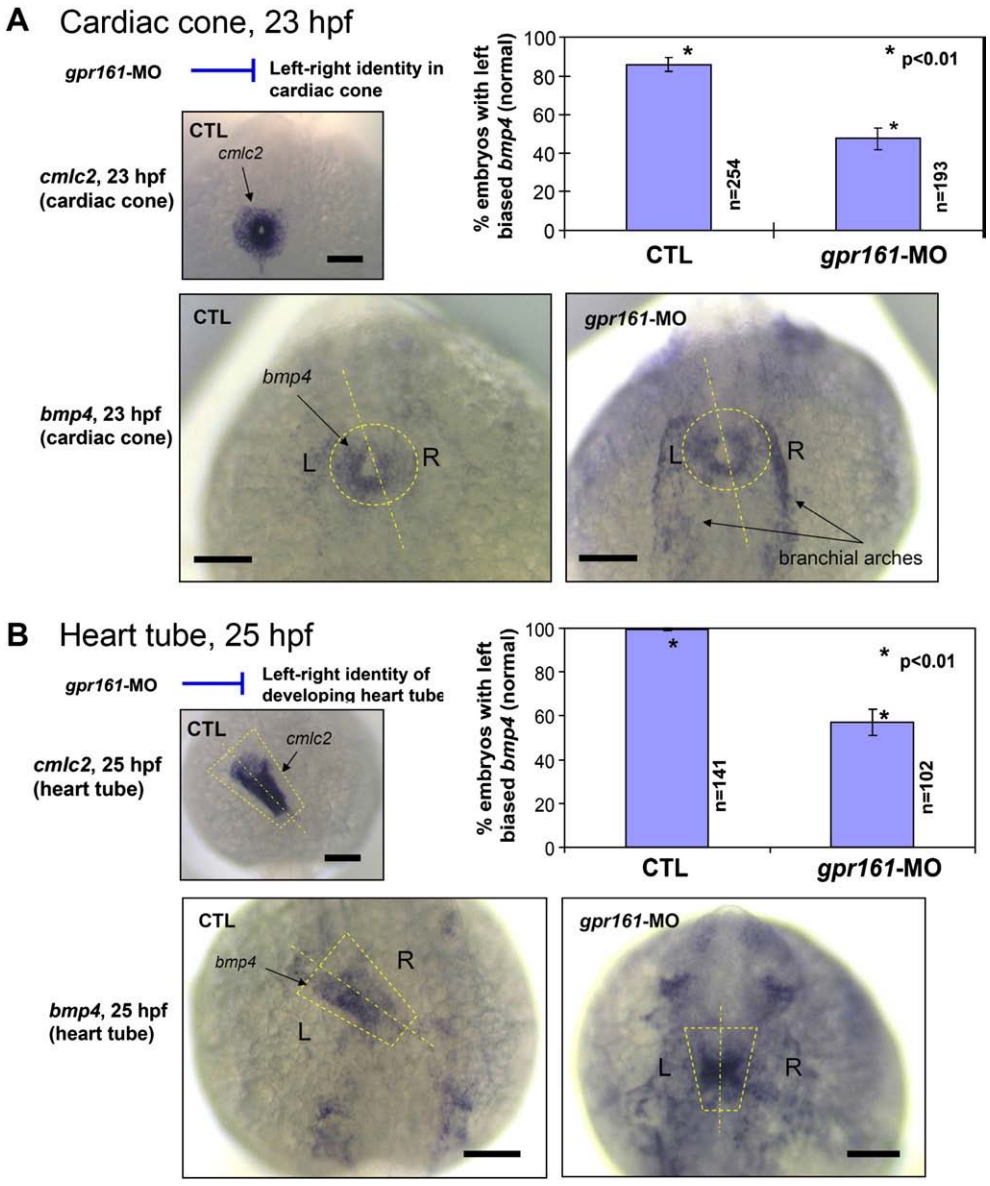

Fig. 4. (A) *bmp4* expression was predominantly on the left side of the cardiac cone in comparison to the uniform expression of *cmlc2* (inset) which was disrupted in *gpr161* knockdown embryos. Graphical summary of control (85.8±3.7%; $n=254$), *gpr161* knockdown (MO#24, 47.5±5.7%; $n=193$) and *t*-test ($p<0.01$) results were from 7 injection experiments. (B) *bmp4* expression was predominantly on the left side of the heart tube in comparison to the uniform expression of *cmlc2* (inset) was disrupted in *gpr161* knockdown embryos. Graphical summary of control (99.5±1.3%; $n=141$), *gpr161* knockdown (MO#24, 56.9±5.9%; $n=102$) and *t*-test ($p<0.01$) results were from 4 injection experiments. Dashed lines were drawn over the cardiac cone and heart tube and the midline of the structures. *n* was number of total embryos. Error bars were ±SEM. All scale bars were 100 μm.

Collectively, these results indicate that L–R patterning in the developing heart tube is perturbed in the majority of *gpr161* knockdown embryos. Given the importance of L–R asymmetry for proper positioning of the heart tube, a primary defect in this process is the most likely explanation for the cardiac defect that was observed in *gpr161* knockdown embryos.

In addition to the heart, morphological L–R asymmetry of the visceral organs is also observed in zebrafish embryos (Horne-Badovinac et al., 2003). Between 26 and 30 hpf, the gut primordium starts to loop, with the liver bud curving to the left and the pancreatic bud occupying an asymmetric position on the right side of the gut. To determine if L–R asymmetry of the visceral organs is affected in *gpr161* knockdown embryos, we used a pan-endodermal marker *foxa3,* which marks the developing gut primordium, including the liver and pancreatic buds (Odenthal and Nusslein-Volhard, 1998; Horne-Badovinac et al., 2003). As expected, 99.3% of control embryos exhibited a leftward budding of the liver and a rightward budding of the pancreas at 36 hpf (Figs. 5A, B). By contrast, the majority of *gpr161* knockdown embryos failed to show normal L–R asymmetry of the visceral organs, with 49.1% embryos exhibiting symmetrical placement of the liver and pancreas with respect to the midline and 11.4% embryos showing heterotaxic phenotypes (Figs. 5B, C; Supplementary Table 5). RNA rescue experiments showed that *gpr161*-RNA can suppress the visceral organ defects from 60.4% to 36.5% in *gpr161* knockdown embryos (Figs. 5B, C; Supplementary Table 5). The L–R orientation of brain, heart, and gut is thought to be regulated by distinct pathways affecting different steps along the anterior–posterior axis of the embryos (Bisgrove et al., 2000). Since *gpr161* knockdown embryos showed severe reduction of *lefty2* and *spaw* expression and exhibited defects in both cardiac looping and visceral organ asymmetry, our results suggest that *gpr161* plays a critical role in the establishment of L–R asymmetry at an early step.

gpr161 knockdown perturbs Ca^{2+} handling surrounding the Kupffer's vesicle

Several recent studies suggest that L–R asymmetry may be controlled by a ciliated organ called the embryonic node in mice, Hensen's node in chick, or Kupffer's vesicle in zebrafish (Hirokawa et al., 2006; Oishi et al., 2006). In the latter, motile cilia are thought to generate a leftward nodal flow that stimulates sensory cilia on cells lining the Kupffer's vesicle (Delmas, 2004; Nauli and Zhou, 2004; Tabin and Vogan, 2003). This process is thought to establish an asymmetric Ca^{2+} signal that produces the asymmetric gene expression (Essner et al., 2005; McGrath et al., 2003; Sarmah et al., 2005). Consistent with a critical role for these cilia, mutations or knockdown of components such as *dynein* have been linked to defective L–R patterning and polycystic kidney disease (Otto et al., 2003; Sun et al., 2004; Kramer-Zucker et al., 2005; Obara et al., 2006).

Consistent with a possible role in the Kupffer's vesicle, zebrafish *gpr161* is expressed in the posterior mesoderm surrounding this structure during early somitogenesis (14 hpf) (Fig. 1B). Moreover, comparative analysis of zebrafish *gpr161* knockdown and the ciliary *dynein* knockdown (Essner et al., 2005) phenotypes reveals some similarities, including absent or altered *lefty1/2* expression. To investigate if *gpr161* function is required for either the formation of the Kupffer's vesicle or expression of cilia, we used confocal imaging to visualize tubulin staining of the cilia on cells lining the Kupffer's vesicle. As compared to the control embryos, *gpr161* knockdown embryos showed no significant difference in the number or morphology of cilia (Supplementary Fig. 4B). Moreover, in contrast to *dynein* knockdown embryos, cystic kidneys were not observed in *gpr161* knockdown embryos, suggesting no apparent defect in the motility of cilia. Thus, despite some similarities, there are obvious differences between *gpr161* and *dynein* knockdown phenotypes, suggesting they may affect different steps in this process. In this regard, we found that *gpr161* may be affecting the generation of the Ca^{2+} signal within cells lining the Kupffer's vesicle. To monitor the Ca^{2+} signal *in vivo*, we injected Ca^{2+} green indicator into 1-cell stage zebrafish embryos to allow even distribution to all embryonic cells, as described previously (Reinhard et al., 1995; Cox and Fetcho, 1996; O'Malley et al., 1996; Nicolson et al., 1998; Fuss and Korsching, 2001; Takahashi et al., 2002; Liu et al., 2003; Webb and Miller, 2003; Sarmah et al., 2005). Using fluorescence microscopy, we detected elevated Ca^{2+} levels in cells surrounding the Kupffer's vesicle in *gpr161* knockdown embryos at 14 hpf (3- to 6-somite stage) (Fig. 6A; Supplementary Fig. 6). Combining histogram analysis of the Ca^{2+} imaging (Supplementary Fig. 6) and mathematical modeling (Supplementary Fig. 7), we

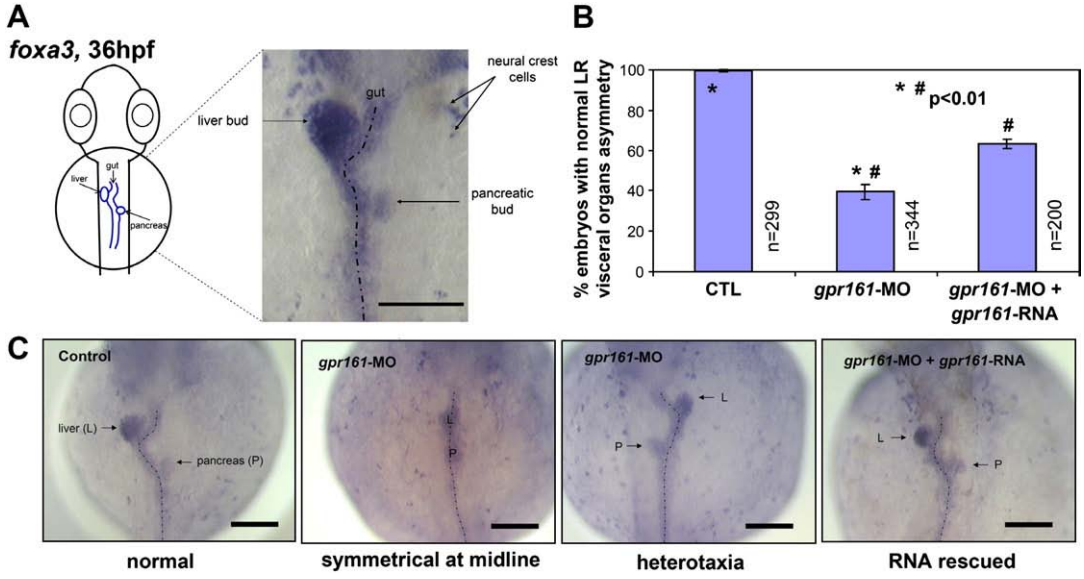

Fig. 5. L–R asymmetry of visceral organs in zebrafish embryos. (A) *foxa3* expression marks the gut primordium at 36 hpf showing the liver bud (left) and pancreatic bud (right) in control embryo. (B) Graphical summary of normal visceral asymmetry in control (97.8±1.3%), *gpr161* knockdown (32.4±4.1%) and RNA rescued (52.2±3.4%) embryos. *t*-test ($p<0.01$) results were from 6 injection experiments. *n* was number of total embryos. Error bars were ±SEM. (C) *foxa3* expression of liver and pancreatic buds in normal L–R asymmetric position in control, symmetric or heterotaxia in *gpr161* knockdown and normal L–R asymmetry in RNA rescued embryos. All scale bars were 100 μm.

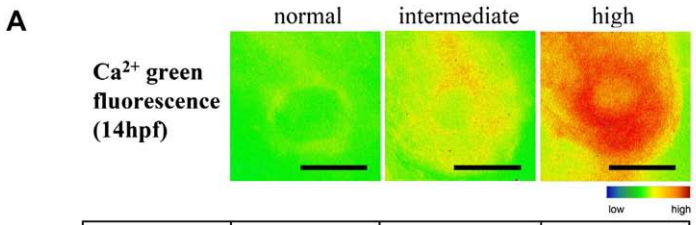

	% Normal	% Intermediate	% High
CTL	100%	0%	0%
gpr161-MO	0%	62%	38%
gpr161-MO + *ncx*-RNA	30%	47%	23%
gpr161-MO + *pmca*-RNA	30%	48%	22%

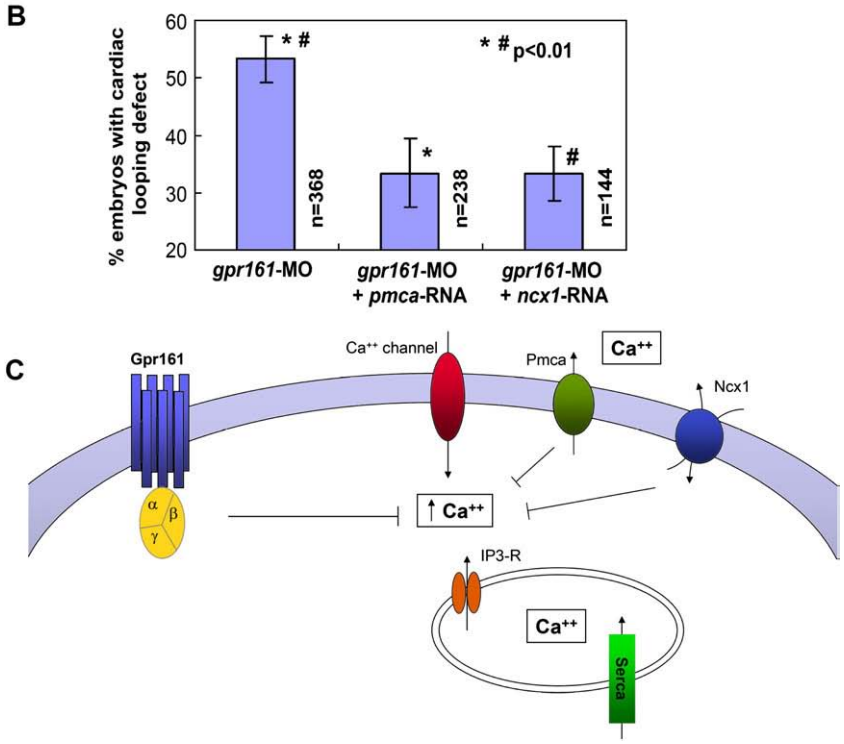

Fig. 6. *gpr161* knockdown disrupts Ca^{2+} handling which is essential for establishment of L–R asymmetry. (A) Defective Ca^{2+} handling resulting in elevated intracellular Ca^{2+} in *gpr161* knockdown embryos surrounding the Kupffer's vesicle. Pseudocolour scale for the intracellular Ca^{2+} signal as normal, intermediate and high intensity. The percentage of embryos exhibited such level of Ca^{2+} signal was listed in control, *gpr161* knockdown, *ncx1*- and *pmca*-RNA rescue of the *gpr161* knockdown embryos. (B) Removal of excessive Ca^{2+} by over-expression of 1 pg of Ca^{2+} pump *pmca* or Na^+/Ca^{2+} exchanger *ncx1* can rescue *gpr161* knockdown phenotype. Cardiac looping defect in *gpr161*-MO (MO#24, 54.1±4.0%; $n=368$), rescued by *pmca*-RNA (32.0±6.0%; $n=238$), rescued by *ncx1*-RNA (34.0±4.8%; $n=144$) and results were from 4 injection experiments. n was number of total embryos. Error bars were ±SEM. t-test * and # indicated statistical significance, $p<0.01$. All scale bars were 100 μm. (C) A model of *gpr161* involved in Ca^{2+} handling and essential for L–R asymmetry for cardiac morphogenesis and visceral asymmetry in developing zebrafish embryos. Blocking *gpr161* function led to defect in Ca^{2+} handling and resulted in elevated free cytosolic Ca^{2+} and loss of cardiac looping and abnormal chamber morphogenesis. The *gpr161* knockdown can be rescued by removing excessive cytosolic free Ca^{2+} using over-expression of Ca^{2+} pump *pmca* and Na^+/Ca^{2+} exchanger *ncx1*.

quantitated the fraction of embryos showing normal, intermediate, and high Ca^{2+} signals in each group. Compared to control embryos, virtually 100% of the *gpr161* knockdown embryos showed intermediate to high Ca^{2+} levels (Fig. 6A). To determine if removal of excess Ca^{2+} can rescue the L–R defect that produced the cardiac looping abnormality in *gpr161* knockdown embryos, we over-expressed the membrane Ca^{2+} pump *pmca,* or the Na^+/Ca^{2+} exchanger *ncx1* (Ebert et al., 2005; Langenbacher et al., 2005). Again, combining histogram analysis of the Ca^{2+} imaging (Supplementary Fig. 6) and mathematical modeling (Supplementary Fig. 7), we showed that injection of either *ncx1* or *pmca*-RNA can normalize Ca^{2+} levels in ~30% of *gpr161* knockdown embryos (Fig. 6A), with correlation coefficients of 0.997 in control, 0.995 in *gpr161* knockdown, 0.993 in *ncx1*-RNA rescue and 0.979 in *pmca*-RNA rescue experiments, respectively. Notably, the percentage of *gpr161* knockdown embryos whose Ca^{2+} levels can be normalized by RNA injection (Fig. 6A) was similar to the percentage of *gpr161* knockdown embryos whose cardiac looping defects can be rescued by RNA injection (Fig. 6B; Supplementary Table 6). Collectively, these findings demonstrate that zebrafish *gpr161* signaling is essential for the regulation of Ca^{2+} levels that are necessary for establishment of L–R asymmetry at an early somite stage. In support of our findings, knockdown of the zebrafish Na^+/Ca^{2+} exchanger *ncx4a* was shown to disrupt Ca^{2+} homeostasis and perturbed L–R patterning via Ca^{2+}/calmodulin-dependent protein kinase (Shu et al., 2007).

Discussion

The analysis of the human genome has revealed ~150 family members that are currently classified as orphan GPCRs due to the lack of information regarding their physiological ligands and functions (Vassilatis et al., 2003; Wise et al., 2004). Because orphan GPCRs represent a potential resource for future drug development, various approaches, including transgenic and gene knockout approaches in mice, have been used to decipher their biological roles (Ma and Zemmel, 2002; Marchese et al., 1999; Rohrer and Kobilka 1998). Nevertheless, progress on identifying biological functions has been slow due to the time consuming and expensive nature of these approaches (Katugampola and Davenport, 2003). Here, we show the utility of combining a RNA knockdown strategy with the rapid developmental program of zebrafish to identify a critical role for the orphan GPCR, *gpr161*, in vertebrate development. These results add to the growing list of GPCRs that have recently been shown to play critical roles in developmental processes (Kupperman et al., 2000; Leung et al., 2006; Yi et al., 2006).

A highly conserved feature of vertebrate development is the establishment of the L–R axis that determines asymmetric placement of the brain, heart, and visceral organs with respect to the embryonic midline. Although not universally accepted (Levin and Palmer, 2007), one model suggests that this process is controlled by motile cilia of the mouse embryonic node or the zebrafish Kupffer's vesicle that create a leftward flow of fluid (Hirokawa et al., 2006; Oishi et al., 2006). Disrupting the formation/function of these cilia blocks fluid flow and causes L–R patterning defects (McGrath et al., 2003; Oishi et al., 2006; Speder et al., 2007; Tabin and Vogan, 2003). Although the underlying mechanism is still emerging, this process seems to involve asymmetric Ca^{2+} flux in the cells surrounding the node/Kupffer's vesicle (Raya et al., 2004; Sarmah et al., 2005; Shimeld, 2004; Speder et al., 2007). This asymmetric Ca^{2+} signal appears to result from activation of polycystin cation channels in the sensory cilia in response to leftward fluid flow produced by the motile cilia (Delmas, 2004; Nauli and Zhou, 2004; Tabin and Vogan, 2003). Perturbing this asymmetric Ca^{2+} signal disrupts left-sided expression of genes such as *spaw* and *lefty2* in the lateral plate mesoderm (Essner et al., 2005; McGrath et al., 2003; Sarmah et al., 2005) and produces L–R patterning defects.

Little is known about the potential role of GPCR signaling pathways in regulating the asymmetric Ca^{2+} signal. Here, we present four lines of evidence supporting the hypothesis that *gpr161* is essential for Ca^{2+} signaling in the Kupffer's vesicle and for determination of the L–R axis. Firstly, *gpr161* is expressed in the posterior and lateral plate mesoderm in close proximity to the developing Kupffer's vesicle- consistent with its role in this process. Secondly, knockdown of *gpr161* results in L–R patterning defects, including abnormalities in cardiac looping and positioning of visceral organs. Thirdly, knockdown of *gpr161* disrupts left-sided expression of laterality genes, including *lefty2* and *spaw* in the lateral plate mesoderm and *bmp4* in the developing heart tube. Lastly, knockdown of *gpr161* produces elevated Ca^{2+} levels in the posterior mesoderm surrounding the Kupffer's vesicle. Collectively, these results support a model in which *gpr161* regulates L–R asymmetry by modulating Ca^{2+} levels in cells surrounding the Kupffer's vesicle. Since fluorescent measurement of Ca^{2+} levels can be affected by pH, we cannot rule out an additional involvement of *gpr161* in regulating pH levels. However, the finding that over-expression of the membrane Ca^{2+} pump *pmca,* or the Na^{+}/Ca^{2+} exchanger *ncx1* normalizes the fluorescent signals and rescues cardiac looping defects in a similar percentage of *gpr161* knockdown embryos strongly suggests a primary role in regulating Ca^{2+} homeostasis.

The signaling pathway(s) acting downstream of *gpr161* has not been identified. However, a computational program (Proteome Alliance: http://tp12.pzr.uni-rostock.de/~moeller/7tmhmm/submission.php) based on structural characteristics of known GPCRs (Möller et al., 2001; Sgourakis et al., 2005) predicts that zebrafish Gpr161 is coupled to a member of the G protein αq family. Members of the Gαq family have been shown to activate phospholipase C-β, which produces diacylglycerol (DAG) and inositol 1,4,5-trisphosphate (IP3). Upon acute activation, IP3 increases the cytosolic Ca^{2+} level by mediating its release from intracellular stores (Hubbard and Hepler, 2006). Subsequently, the intracellular stores are replenished by increasing entry of extracellular Ca^{2+} across the plasma membrane. However, upon chronic stimulation, DAG acting via protein kinase C is thought to prevent Ca^{2+} overload by inhibiting the entry of extracellular Ca^{2+} (Fan et al., 2005; Lu et al., 2005; Sternfeld et al., 2007). We envision that the zebrafish Gpr161 may act in a similar fashion. Accordingly, we propose a model in which the zebrafish orphan receptor Gpr161 reduces Ca^{2+} entry through the plasma membrane by inhibiting a Ca^{2+} channel, Ca^{2+} pump, or Ca^{2+} exchanger (Fig. 6C). Further supporting a role for inositol phosphate signaling in L–R axis determination, knockdown of an inositol phosphate kinase (*ipk1*) has been shown to interfere with asymmetric Ca^{2+} flux and produce L–R patterning defects (Sarmah et al., 2005). Since *gpr161* is expressed in the posterior mesoderm, this signaling pathway may function in the cells surrounding the Kupffer's vesicle. Alternatively, this signaling pathway may function in the dorsal forerunner cells giving rise to this structure (Schneider et al., 2008). Although future studies will be needed to clarify the signaling pathway and identify the earliest site of its action, our results show that the orphan GPCR, *gpr161*, is critical for the establishment of L–R asymmetry through direct or indirect regulation of Ca^{2+} homeostasis in zebrafish.

Although a previous report has identified a requirement for a G protein in the initiation of L–R patterning in invertebrates (Bergmann et al., 2003), this is the first report of a GPCR acting in the elaboration and maintenance of L–R patterning in vertebrates. Considering the conservation of molecular components in L–R asymmetry and cardiac morphogenesis, it will be of interest to investigate if the *gpr161* signaling pathway is similarly involved in establishment of the L–R axis in mammals. While this paper was under revision, a study appeared linking a probable gain-of-function mutation of mouse *Gpr161* gene to abnormal neural fold closure and lens development in mice (Matteson et al., 2008). Taken together, the finding that knockdown phenotypes result from loss-of-function of *gpr161* in zebrafish as well as gain-of-function in mice supports an evolutionarily conserved role in vertebrate development.

Materials and methods

Zebrafish, Danio rerio

Florida wildtype strain ('That Fish Place', Lancaster, Pennsylvania). Longfin strain (Scientific Hatcheries, Huntington Beach, CA). Transgenic zebrafish line (*TG[cmlc:GFP]*) (Huang et al., 2003).

RNA over-expression

Zebrafish *gpr161* over-expression construct was generated by PCR using primers (listed below) and then subcloned into pCS^{2+} vector at BamH1/Xho1 and Cla1/Xho1 sites, respectively. Capped sense RNA was synthesized using SP6 RNA polymerase and the mMESSAGE mMACHINE system (Ambion, Austin, TX). Canine *ncx1* was kindly provided by Dr. Ken Philipson and zebrafish *pmca* was kindly provided by Dr. Jau-Nian Chen. For microinjection of *gpr161*, *ncx1* and *pmca* mRNA or morpholino antisense oligos, zebrafish embryos were injected at 1 cell stage with injection volume of about 0.5 nl, subsequently incubated in 0.3× Danieau's medium at 28.5 °C. Embryos were maintained in the above condition until they reached different developmental stages for total RNA preparation and whole

mount in situ hybridization. PCR primers for the *gpr161*-RNA construct were:

*gpr161*FL-F1: 5′-AATGAACGGCTCTAAGAATGGGACG;
*gpr161*FL-R1: 5′-CTGTACCTTCAAAAGCTGCAGATTAAA.

Antisense morpholino oligos

gpr161-MO (translational blocking antisense morpholinos) synthesized by GeneTools, LLC, Philomath, Oregon:

(MO#24, targeting at ATG start codon): 5′-CGTCCCATTCTTAGAGCCGTTCATT; (MO#36, targeting at 5′UTR): 5′-GAGGCTTCTGGTTGCCAATGACTTG.
5-mismatch-MO control (MO#28): 5′-CCTCCGATTGTTAGAGCCCTTGATT (mismatch were underlined).

For *gpr161* RNA rescue experiment, MO#36 targeting the 5′UTR was used. For all other experiments, MO#24 targeting the ATG start codon was used. Morpholinos were injected into zebrafish embryos at 1 cell stage with injection volume of about 0.5 nl at 100 μM and 300 μM for MO#24 and MO#36, respectively. Zebrafish *gpr161* acc. no. (EU090912).

Whole mount in situ hybridization

Details of the whole mount in situ hybridization protocol and probes used in this study are given in Supplementary data.

RT-PCR

Details of the RT-PCR protocol and primers for *gpr161* and *actin* are provided in the Supplementary data.

Detection of MO blocking function by in vitro system

An in vitro transcription and translation coupled system to assay the efficacy and specificity of the MO is described in the Supplementary data.

Detection of intracellular Ca^{2+} in zebrafish embryos

Ca^{2+} green-dextran 10,000 MW (Molecular probe/Invitrogen, Carlsbad, CA) was used at 0.05% (w/v) for microinjection into zebrafish embryos at 1 cell stage of injection volume of about 0.5 nl. Embryos were incubated in 0.3× Danieau's medium at 28.5 °C. Fluorescent image at 500 ms exposure of the Kupffer's vesicle (KV) at 3 to 6-somite stage was documented using a MZFL3 stereomicroscope with GFP Plus fluorescence filter set of excitation filter 480/40 nm and barrier filter 510 nm (Leica Microsystems, Wetzlar, Germany) and images were converted equally to an intensity scale using ImagePro+ software (Media Cybernetics, Silver Spring, MD; red indicating high intensity; yellow, moderate; green, low).

Acknowledgments

We are grateful to Drs. Deborah Yelon, Jau-Nian Chen, Ken Philipson, Michael Rebagliati, Matthais Hammerschmidt and Wolfgang Driever for sharing reagents; Dr. William Schwindinger for mathematical modeling of histogram analysis and Dr. Carl Hansen for valuable suggestion on the analysis; and Cynthia Rhone, Gail Gregory, Shannon Wescott and Steven Krasucki for animal care. We thank Drs. Jau-Nian Chen and William Schwindinger, and Soniya Sinha for critical review of the manuscript. We are very thankful to our editorial reviewers that gave us the critical comments and suggestions in our manuscript. This study is funded by NIH grants GM58191 and GM39867 awarded to JDR. While this paper was being prepared for submission, an online version of a paper describing a hypomorphic allele of mouse *Gpr161* gene with congenital cataracts and neural tube defects was published (Matteson et al., 2008).

Appendix A. Supplementary data

Supplementary data associated with this article can be found, in the online version, at doi:10.1016/j.ydbio.2008.08.001.

References

Amsterdam, A., Burgess, S., Golling, G., Chen, W., Sun, Z., Townsend, K., Farrington, S., Haldi, M., Hopkins, N., 1999. A large-scale insertional mutagenesis screen in zebrafish. Genes Dev. 13, 2713–2724.
Bergmann, D.C., Lee, M., Robertson, B., Tsou, M.F., Rose, L.S., Wood, W.B., 2003. Embryonic handedness choice in *C. elegans* involves the Galpha protein GPA-16. Development 130, 5731–5740.
Bisgrove, B.W., Essner, J.J., Yost, H.J., 2000. Multiple pathways in the midline regulate concordant brain, heart and gut left–right asymmetry. Development 127, 3567–3579.
Chen, J.N., Fishman, M.C., 1996. Zebrafish tinman homolog demarcates the heart field and initiates myocardial differentiation. Development 122, 3809–3816.
Chen, J.N., van Eeden, F.J., Warren, K.S., Chin, A., Nusslein-Volhard, C., Haffter, P., Fishman, M.C., 1997. Left–right pattern of cardiac BMP4 may drive asymmetry of the heart in zebrafish. Development 124, 4373–4382.
Chocron, S., Verhoeven, M.C., Rentzsch, F., Hammerschmidt, M., Bakkers, J., 2007. Zebrafish Bmp4 regulates left–right asymmetry at two distinct developmental time points. Dev. Biol. 305, 577–588.
Cox, K.J., Fetcho, J.R., 1996. Labeling blastomeres with a calcium indicator: a non-invasive method of visualizing neuronal activity in zebrafish. J. Neurosci. Methods 68, 185–191.
Delmas, P., 2004. Polycystins: from mechanosensation to gene regulation. Cell 118, 145–148.
Driever, W., Solnica-Krezel, L., Schier, A.F., Neuhauss, S.C., Malicki, J., Stemple, D.L., Stainier, D.Y., Zwartkruis, F., Abdelilah, S., Rangini, Z., Belak, J., Boggs, C., 1996. A genetic screen for mutations affecting embryogenesis in zebrafish. Development 123, 37–46.
Ebert, A.M., Hume, G.L., Warren, K.S., Cook, N.P., Burns, C.G., Mohideen, M.A., Siegal, G., Yelon, D., Fishman, M.C., Garrity, D.M., 2005. Calcium extrusion is critical for cardiac morphogenesis and rhythm in embryonic zebrafish hearts. Proc. Natl. Acad. Sci. U. S. A. 102, 17705–17710.
Essner, J.J., Amack, J.D., Nyholm, M.K., Harris, E.B., Yost, H.J., 2005. Kupffer's vesicle is a ciliated organ of asymmetry in the zebrafish embryo that initiates left–right development of the brain, heart and gut. Development 132, 1247–1260.
Fan, G., Jiang, Y.P., Lu, Z., Martin, D.W., Kelly, D.J., Zuckerman, J.M., Ballou, L.M., Cohen, I.S., Lin, R.Z., 2005. A transgenic mouse model of heart failure using inducible Galpha q. J. Biol. Chem. 280, 40337–40346.
Fraser, L.R., Adeoya-Osiguwa, S.A., Baxendale, R.W., 2003. First messenger regulation of capacitation via G protein-coupled receptors. Mol. Hum. Reprod. 9, 739–748.
Fredriksson, R., Schioth, H.B., 2005. The repertoire of G-protein-coupled receptors in fully sequenced genomes. Mol. Pharmacol. 67, 1414–1425.
Fredriksson, R., Lagerstrom, M.C., Lundin, L.G., Schioth, H.B., 2003. The G-protein-coupled receptors in the human genome form five main families. Phylogenetic analysis, paralogon groups, and fingerprints. Mol. Pharmacol. 63, 1256–1272.
Fuss, S.H., Korsching, S.I., 2001. Odorant feature detection: activity mapping of structure response relationships in the zebrafish olfactory bulb. J. Neurosci. 21, 8396–8407.
Geisler, R., Rauch, G.J., Geiger-Rudolph, S., Albrecht, A., van Bebber, F., Berger, A., Busch-Nentwich, E., Dahm, R., Dekens, M.P., Dooley, C., Elli, A.F., Gehring, I., Geiger, H., Geisler, M., Glaser, S., Holley, S., Huber, M., Kerr, A., Kirn, A., Knirsch, M., Konantz, M., Küchler, A.M., Maderspacher, F., Neuhauss, S.C., Nicolson, T., Ober, E.A., Praeg, E., Ray, R., Rentzsch, B., Rick, J.M., Rief, E., Schauerte, H.E., Schepp, C.P., Schönberger, U., Schonthaler, H.B., Seiler, C., Sidi, S., Söllner, C., Wehner, A., Weiler, C., Nüsslein-Volhard, C., 2007. Large-scale mapping of mutations affecting zebrafish development. BMC Genomics 8, 11.
Griffin, C.T., Srinivasan, Y., Zheng, Y.W., Huang, W., Coughlin, S.R., 2001. A role for thrombin receptor signaling in endothelial cells during embryonic development. Science 293, 1666–1670.
Haffter, P., Granato, M., Brand, M., Mullins, M.C., Hammerschmidt, M., Kane, D.A., Odenthal, J., van Eeden, F.J., Jiang, Y.J., Heisenberg, C.P., Kelsh, R.N., Furutani-Seiki, M., Vogelsang, E., Beuchle, D., Schach, U., Fabian, C., Nüsslein-Volhard, C., 1996. The identification of genes with unique and essential functions in the development of the zebrafish, *Danio rerio*. Development 123, 1–36.
Heisenberg, C.P., Tada, M., Rauch, G.J., Saude, L., Concha, M.L., Geisler, R., Stemple, D.L., Smith, J.C., Wilson, S.W., 2000. Silberblick/Wnt11 mediates convergent extension movements during zebrafish gastrulation. Nature 405, 76–81.
Hirokawa, N., Tanaka, Y., Okada, Y., Takeda, S., 2006. Nodal flow and the generation of left–right asymmetry. Cell 125, 33–45.
Horne-Badovinac, S., Rebagliati, M., Stainier, D.Y., 2003. A cellular framework for gut-looping morphogenesis in zebrafish. Science 302, 662–665.
Huang, C.J., Tu, C.T., Hsiao, C.D., Hsieh, F.J., Tsai, H.J., 2003. Germ-line transmission of a myocardium-specific GFP transgene reveals critical regulatory elements in the cardiac myosin light chain 2 promoter of zebrafish. Dev. Dyn. 228, 30–40.

Hubbard, K.B., Hepler, J.R., 2006. Cell signaling diversity of the Gqalpha family of heterotrimeric G proteins. Cell. Signal. 18, 135–150.
Katugampola, S., Davenport, A., 2003. Emerging roles for orphan G-protein-coupled receptors in the cardiovascular system. Trends Pharmacol. Sci. 24, 30–35.
Kramer-Zucker, A.G., Olale, F., Haycraft, C.J., Yoder, B.K., Schier, A.F., Drummond, I.A., 2005. Cilia-driven fluid flow in the zebrafish pronephros, brain and Kupffer's vesicle is required for normal organogenesis. Development 132, 1907–1921.
Krogh, A., Larsson, B., von Heijne, G., Sonnhammer, E.L.L., 2001. Predicting transmembrane protein topology with a hidden Markov model: application to complete genomes. J. Mol. Biol. 305, 567–580.
Kupperman, E., An, S., Osborne, N., Waldron, S., Stainier, D.Y., 2000. A sphingosine-1-phosphate receptor regulates cell migration during vertebrate heart development. Nature 406, 192–195.
Langenbacher, A.D., Dong, Y., Shu, X., Choi, J., Nicoll, D.A., Goldhaber, J.I., Philipson, K.D., Chen, J.N., 2005. Mutation in sodium–calcium exchanger 1 (NCX1) causes cardiac fibrillation in zebrafish. Proc. Natl. Acad. Sci. U. S. A. 102, 17699–17704.
Leung, T., Chen, H., Stauffer, A.M., Giger, K.E., Sinha, S., Horstick, E.J., Humbert, J.E., Hansen, C.A., Robishaw, J.D., 2006. Zebrafish G protein gamma2 is required for VEGF signaling during angiogenesis. Blood 108, 160–166.
Levin, M., Palmer, A.R., 2007. Left–right patterning from the inside out: widespread evidence for intracellular control. Bioessays 29, 271–287.
Liu, K.S., Gray, M., Otto, S.J., Fetcho, J.R., Beattie, C.E., 2003. Mutations in deadly seven/notch1a reveal developmental plasticity in the escape response circuit. J. Neurosci. 23, 8159–8166.
Lin, F., Sepich, D.S., Chen, S., Topczewski, J., Yin, C., Solnica-Krezel, L., Hamm, H., 2005. Essential roles of Ga12/13 signaling in distinct cell behaviors driving zebrafish convergence and extension gastrulation movements. J. Cell Biol. 169, 777–787.
Long, S., Ahmad, N., Rebagliati, M., 2003. The zebrafish nodal-related gene southpaw is required for visceral and diencephalic left–right asymmetry. Development 130, 2303–2316.
Lu, Z., Jiang, Y.P., Ballou, L.M., Cohen, I.S., Lin, R.Z., 2005. Galpha q inhibits cardiac L-type Ca^{2+} channels through phosphatidylinositol 3-kinase. J. Biol. Chem. 280, 40347–40354.
Ma, P., Zemmel, R., 2002. Value of novelty? Nat. Rev. Drug Discov. 1, 571–572.
Marchese, A., George, S.R., Kolakowski Jr, L.F., Lynch, K.R., O'Dowd, B.F., 1999. Novel GPCRs and their endogenous ligands: expanding the boundaries of physiology and pharmacology. Trends Pharmacol. Sci. 20, 370–375.
Matteson, P.G., Desai, J., Korstanje, R., Lazar, G., Borsuk, T.E., Rollins, J., Kadambi, S., Joseph, J., Rahman, T., Wink, J., Benayed, R., Paigen, B., Millonig, J.H., 2008. The orphan G protein-coupled receptor, Gpr161, encodes the vacuolated lens locus and controls neurulation and lens development. Proc. Natl. Acad. Sci. U. S. A. 105, 2088–2093.
McGrath, J., Somlo, S., Makova, S., Tian, X., Brueckner, M., 2003. Two populations of node monocilia initiate left–right asymmetry in the mouse. Cell 114, 61–73.
Möller, S., Vilo, J., Croning, M.D., 2001. Prediction of the coupling specificity of G protein coupled receptors to their G proteins. Bioinformatics 17, S174–S181.
Nasevicius, A., Ekker, S.C., 2000. Effective targeted gene 'knockdown' in zebrafish. Nat. Genet. 26, 216–220.
Nauli, S.M., Zhou, J., 2004. Polycystins and mechanosensation in renal and nodal cilia. Bioessays 26, 844–856.
Nicolson, T., Rüsch, A., Friedrich, R.W., Granato, M., Ruppersberg, J.P., Nüsslein-Volhard, C., 1998. Genetic analysis of vertebrate sensory hair cell mechanosensation: the zebrafish circler mutants. Neuron 20, 271–283.
O'Malley, D.M., Kao, Y.-H., Fetcho, J.R., 1996. Imaging the functional organization of zebrafish hindbrain segments during escape behaviors. Neuron 17, 1145–1155.
Obara, T., Mangos, S., Liu, Y., Zhao, J., Wiessner, S., Kramer-Zucker, A.G., Olale, F., Schier, A.F., Drummond, I.A., 2006. Polycystin-2 immunolocalization and function in zebrafish. J. Am. Soc. Nephrol. 17, 2706–2718.
Odenthal, J., Nusslein-Volhard, C., 1998. Fork head domain genes in zebrafish. Dev. Genes Evol. 208, 245–258.
Offermanns, S., Mancino, V., Revel, J.P., Simon, M.I., 1997. Vascular system defects and impaired cell chemokinesis as a result of Ga13 deficiency. Science 275, 533–536.
Oishi, I., Kawakami, Y., Raya, A., Callol-Massot, C., Izpisua Belmonte, J.C., 2006. Regulation of primary cilia formation and left–right patterning in zebrafish by a noncanonical Wnt signaling mediator, duboraya. Nat. Genet. 38, 1316–1322.
Otto, E.A., Schermer, B., Obara, T., O'Toole, J.F., Hiller, K.S., Mueller, A.M., Ruf, R.G., Hoefele, J., Beekmann, F., Landau, D., Foreman, J.W., Goodship, J.A., Strachan, T., Kispert, A., Wolf, M.T., Gagnadoux, M.F., Nivet, H., Antignac, C., Walz, G., Drummond, I.A., Benzing, T., Hildebrandt, F., 2003. Mutations in INVS encoding inversin cause nephronophthisis type 2, linking renal cystic disease to the function of primary cilia and left–right axis determination. Nat. Genet. 34, 413–420.
Peterson, R.T., Link, B.A., Dowling, J.E., Schreiber, S.L., 2000. Small molecule developmental screens reveal the logic and timing of vertebrate development. Proc. Natl. Acad. Sci. U. S. A. 97, 12965–12969.
Raya, A., Kawakami, Y., Rodríguez-Esteban, C., Ibañes, M., Rasskin-Gutman, D., Rodríguez-León, J., Büscher, D., Feijó, J.A., Izpisúa-Belmonte, J.C., 2004. Notch activity acts as a sensor for extracellular calcium during vertebrate left–right determination. Nature 427, 121–128.
Reinhard, E., Yokoe, H., Niebling, K.R., Allbritton, N.L., Kuhn, M.A., Meyer, T., 1995. Localized calcium signals in early zebrafish development. Dev. Biol. 170, 50–61.
Rohrer, D.K., Kobilka, B.K., 1998. G protein-coupled receptors: functional and mechanistic insights through altered gene expression. Physiol. Rev. 78, 35–52.
Romo, X., Pastén, P., Martínez, S., Soto, X., Lara, P., de Arellano, A.R., Torrejón, M., Montecino, M., Hinrichs, M.V., Olate, J., 2008. xRic-8 is a GEF for Gsalpha and participates in maintaining meiotic arrest in *Xenopus laevis* oocytes. J. Cell. Physiol. 214, 673–680.
Ruppel, K.M., Willison, D., Kataoka, H., Wang, A., Zheng, Y.W., Cornelissen, I., Yin, L., Xu, S.M., Coughlin, S.R., 2005. Essential role for Ga13 in endothelial cells during embryonic development. Proc. Natl. Acad. Sci. U. S. A. 102, 8281–8286.
Sarmah, B., Latimer, A.J., Appel, B., Wente, S.R., 2005. Inositol polyphosphates regulate zebrafish left–right asymmetry. Dev. Cell 9, 133–145.
Schilling, T.F., Concordet, J.P., Ingham, P.W., 1999. Regulation of left–right asymmetries in the zebrafish by Shh and BMP4. Dev. Biol. 210, 277–287.
Schneider, I., Houston, D.W., Rebagliati, M.R., Slusarski, D.C., 2008. Calcium fluxes in dorsal forerunner cells antagonize beta-catenin and alter left–right patterning. Development 135, 75–84.
Schwartz, T.W., Frimurer, T.M., Holst, B., Rosenkilde, M.M., Elling, C.E., 2006. Molecular mechanism of 7TM receptor activation—a global toggle switch model. Annu. Rev. Pharmacol. Toxicol. 46, 481–519.
Scott, I.C., Masri, B., D'Amico, L.A., Jin, S.W., Jungblut, B., Wehman, A.M., Baier, H., Audigier, Y., Stainier, D.Y., 2007. The G protein-coupled receptor agtrl1b regulates early development of myocardial progenitors. Dev. Cell 12, 403–413.
Sgourakis, N.G., Bagos, P.G., Hamodrakas, S.J., 2005. Prediction of the coupling specificity of GPCRs to four families of G-proteins using hidden Markov models and artificial neural networks. Bioinformatics 21, 4101–4106.
Shimeld, S.M., 2004. Calcium turns sinister in left–right asymmetry. Trends Genet. 20, 277–280.
Shu, X., Huang, J., Dong, Y., Choi, J., Langenbacher, A., Chen, J.N., 2007. Na^+,K^+-ATPase alpha2 and Ncx4a regulate zebrafish left–right patterning. Development 134, 1921–1930.
Speder, P., Petzoldt, A., Suzanne, M., Noselli, S., 2007. Strategies to establish left/right asymmetry in vertebrates and invertebrates. Curr. Opin. Genet. Dev. 17, 1–8.
Sternfeld, L., Duddenhoffer, M., Ludes, A., Heinze, D., Anderie, I., Krause, E., 2007. Activation of muscarinic receptors reduces store-operated Ca^{2+} entry in HEK293 cells. Cell Signal 19, 1457–1464.
Sun, Z., Amsterdam, A., Pazour, G.J., Cole, D.G., Miller, M.S., Hopkins, N., 2004. A genetic screen in zebrafish identifies cilia genes as a principal cause of cystic kidney. Development 131, 4085–4093.
Tabin, C.J., Vogan, K.J., 2003. A two-cilia model for vertebrate left–right axis specification. Genes Dev. 17, 1–6.
Takahashi, M., Narushima, M., Oda, Y., 2002. In vivo imaging of functional inhibitory networks on the mauthner cell of larval zebrafish. J. Neurosci. 22, 3929–3938.
Vassilatis, D.K., Hohmann, J.G., Zeng, H., Li, F., Ranchalis, J.E., Mortrud, M.T., Brown, A., Rodriguez, S.S., Weller, J.R., Wright, A.C., Bergmann, J.E., Gaitanaris, G.A., 2003. The G protein-coupled receptor repertoires of human and mouse. Proc. Natl. Acad. Sci. U. S. A. 100, 4903–4908.
Webb, S.E., Miller, A.L., 2003. Imaging intercellular calcium waves during late epiboly in intact zebrafish embryos. Zygote 11, 175–182.
Wise, A., Jupe, S.C., Rees, S., 2004. The identification of ligands at orphan G-protein coupled receptors. Annu. Rev. Pharmacol. Toxicol. 44, 43–66.
Yelon, D., Horne, S.A., Stainier, D.Y., 1999. Restricted expression of cardiac myosin genes reveals regulated aspects of heart tube assembly in zebrafish. Dev. Biol. 214, 23–37.
Yi, P., Han, Z., Li, X., Olson, E.N., 2006. The mevalonate pathway controls heart formation in Drosophila by isoprenylation of Ggamma1. Science 313, 1301–1303.
Zeng, X.X., Wilm, T.P., Sepich, D.S., Solnica-Krezel, L., 2007. Apelin and its receptor control heart field formation during zebrafish gastrulation. Dev. Cell 12, 391–402.